Received 23 October 2025; Accepted 22 November 2025
https://doi.org/10.48612/letters/2025-4-383-387
https://elibrary.ru/xvmgwa

Simulation of supratransmission effect in nickel

D. V. Bachurin, R. T. Murzaev†

†murzaevrt@gmail.com

Institute for Metals Superplasticity Problems RAS, Ufa 450001, Russia

Abstract: For the first time, molecular dynamics simulations have been employed to investigate energy transfer in a three-dimensional fcc nickel lattice driven harmonically through a pair of neighboring atoms at frequencies lying outside the phonon spectrum. The dependence of the critical driving frequency on the driving amplitude was determined. When the driving frequency is below this threshold, energy is efficiently transmitted from the driven atoms into the lattice, leading to the spontaneous generation and emission of discrete breathers propagating in opposite directions along close-packed atomic rows. In contrast, when the driving frequency exceeds the critical value, energy transfer to the lattice ceases and the supratransmission effect is not observed. These findings provide new insights into nonlinear energy transport mechanisms in crystalline solids and the conditions necessary for the excitation of discrete breathers in three-dimensional metallic lattices.

Keywords: fcc nickel, molecular dynamics simulations, external driving, intrinsic localized mode, nonlinear dynamics

Acknowledgements: *The work was accomplished in terms of the State Assignment of the Institute for Metals Superplasticity Problems of the Russian Academy of Sciences financed by the Ministry of Science and Higher Education of the Russian Federation (Registration No. 124022900108-3).*

1. Introduction

In crystalline lattices, atoms are arranged in an ordered periodic structure, and their interactions are described by potential functions that determine the forces between neighboring particles. If these forces depend nonlinearly on the displacements of atoms from their equilibrium lattice sites, the system is referred to as a nonlinear lattice. Nonlinearity gives rise to unique dynamical phenomena not present in linear systems, including energy localization and the emergence of amplitude-dependent intrinsic oscillatory modes.

A key manifestation of nonlinear lattice dynamics is the discrete breather, also known as an intrinsic localized mode [1–5]. Discrete breathers are spatially localized, time-periodic oscillations of atoms that can concentrate a significant portion of the system's energy in a limited region of the crystal, while the surrounding atoms remain nearly stationary. These excitations can exist in defect-free crystals and influence macroscopic material properties, including thermal expansion [6,7], thermal conductivity [8], and heat capacity [9–15].

Energy transfer in nonlinear lattices occurs through two main mechanisms. First, energy can propagate via extended phonon waves, similar to conventional linear wave excitations. Second, energy can localize and travel in the form of discrete breathers, which may be generated spontaneously or through external driving. When a lattice is driven by a periodic external force at frequencies outside the phonon spectrum, energy cannot propagate via extended waves, but sufficiently strong driving can excite discrete breathers. These localized modes transport energy through the crystal, potentially leading to the phenomenon of supratransmission.

Supratransmission is a nonlinear phenomenon in lattices where energy is transmitted through the system at driving frequencies outside the phonon spectrum. In this regime, conventional phonon waves cannot propagate, and energy transfer occurs only when the driving amplitude exceeds a critical threshold. Above this threshold, the lattice can support the generation of discrete breathers, which carry energy across the lattice in a localized and time-periodic manner. Originally discovered in one-dimensional nonlinear chains, supratransmission provides a mechanism for energy transport in frequency ranges that are otherwise forbidden for linear excitations. This phenomenon is particularly important for understanding energy localization, signal propagation, and the dynamic response of nonlinear crystalline materials.

Beyond its theoretical significance, supratransmission has promising practical applications. It can be utilized for binary information transmission [16], weak signal detection [17], and the generation of asymmetric energy flow in nonlinear systems [18].

Supratransmission effect has been extensively studied in one-dimensional nonlinear lattices, where this phenomenon was first identified and characterized [19–21]. In contrast, investigations in higher-dimensional lattices remain relatively limited. Only a few studies have addressed two-dimensional systems [22–26], while research on three-dimensional lattices is even scarcer [27–29].

While most previous studies have focused on one- and two-dimensional nonlinear lattices, little attention has been given to supratransmission in three-dimensional crystals, where atomic interactions and collective nonlinear dynamics are far more complex. In this work, we investigate for the first time, using molecular dynamics simulations, the supratransmission effect in a three-dimensional fcc nickel lattice driven harmonically through a pair of neighboring atoms at frequencies outside the phonon spectrum.

2. Model and computational methods

Molecular dynamics simulations were performed with the help of LAMMPS software package [30], a widely used tool for atomistic modeling that enables the simulation of a broad range of physical phenomena in materials at the atomic scale [31–35]. The interatomic interactions in fcc nickel were described by an embedded atom method (EAM) potential from the LAMMPS library [36, 37], which accurately reproduces metallic bonding. For nickel, the equilibrium lattice constant at absolute zero was obtained as 3.52 Å.

The computational supercell is a perfect lattice contained 120×10×10 translational cells (46 080 atoms). The Cartesian axes *x*, *y*, and *z* of the supercell were aligned with the crystallographic directions [1$\bar{1}$0], [110], and [001], respectively. The time step is chosen to be 0.5 fs which is small enough to accurately describe the motion of atoms in standard molecular dynamics. The periodic boundary conditions are applied along all the three orthogonal directions of the computational cell. All calculations are carried out at zero initial temperature $T = 0$ K using the NVE (constant number of atoms, volume, and energy) thermodynamic ensemble. Zero temperature is chosen since thermal fluctuations of atoms can significantly hinder the precise conditions required for observation of supratransmission effect. The duration of each simulation was limited to 20 000 timesteps, which is equivalent to 10 ps. This timescale was found to be enough for observation of the phenomena studied.

Energy transfer between objects in a lattice can occur in two principal ways: (i) kinematically, through direct collisions between particles, and (ii) dynamically, by applying an external periodic driving force to the particles. In the present study, the second approach was employed. Specifically, two atoms 1 and 2 located at the center of the computational cell were selected, and external alternating driving forces F_1 and F_2 were applied to them according to the following relations:

$$F_1 = A \cdot \sin(\omega t) \quad \text{and} \quad F_2 = -A \cdot \sin(\omega t),$$

where A and ω denote the driving amplitude and frequency, respectively. In this study, the phase shift between the two applied forces was set equal to zero, ensuring that atoms 1 and 2 oscillate in exact antiphase with respect to each other.

One of the primary challenges in simulating the supratransmission effect is determining the initial conditions under which this nonlinear phenomenon can be observed. To address this, a systematic variation of the initial amplitudes of atomic displacements from their equilibrium lattice sites, as well as the oscillation frequencies, was performed over a wide range of 0.15 – 0.35 Å and 9.91–10.31 THz, respectively. Only two atoms located in the same atomic plane within the computational cell were displaced, while all other atoms were at their equilibrium positions. Furthermore, all atoms were assigned zero initial velocities to eliminate any contribution from pre-existing kinetic energy, allowing the subsequent dynamics to arise solely from the imposed displacements.

3. Results

The two driven particles serve as a localized energy source, and the kinetic energy of the computational cell was evaluated as a function of time for different combinations of driving amplitude A and frequency ω, as presented in Fig. 1. Panels (a) and (b) correspond to driving amplitudes of $A = 0.15$ and 0.28 Å, respectively. At low driving amplitude of 0.15 Å and for frequencies below the upper edge of the phonon spectrum (9.93 THz for the chosen interatomic potential), continuous energy transfer into the system is observed (see Fig. 1a). As a result, the kinetic energy of the system increases

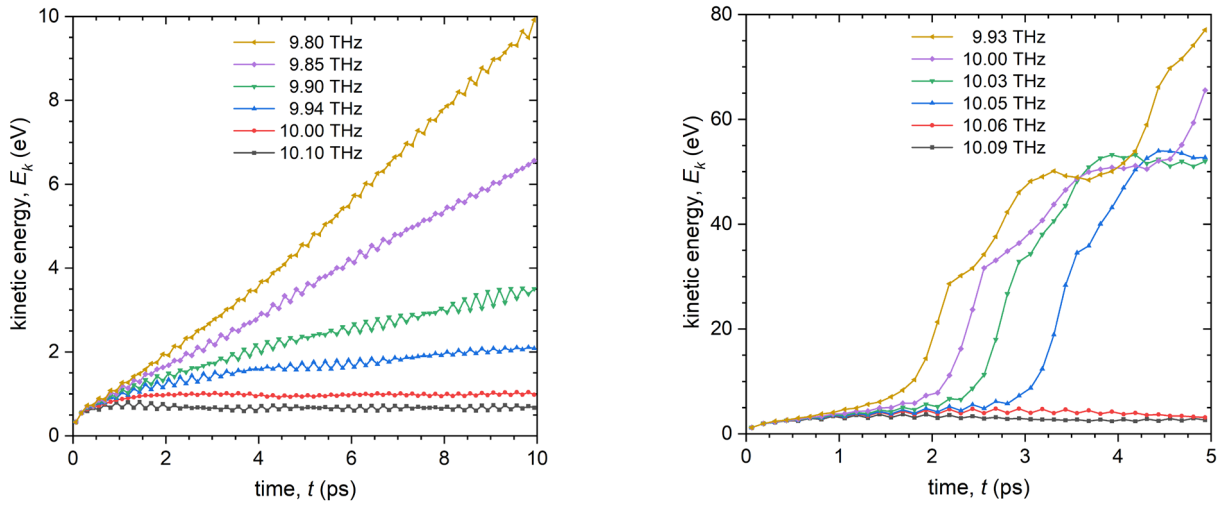

a b

Fig. 1. (Color online) Kinetic energy per atom as a function of time calculated for six different frequencies and for driving amplitudes $A = 0.15$ Å (a) and $A = 0.28$ Å (b). The solid lines connecting the data points are provided as visual guides.

almost linearly with time, particularly within the frequency range of 9.8 – 9.9 THz. When the driving frequency exceeds 9.94 THz, the kinetic energy growth ceases after a certain period and reaches a steady-state value. This saturation indicates that, for frequencies above the upper edge of the phonon spectrum, the energy supplied to the driven atoms by the external alternating force is no longer transmitted to the surrounding lattice. Consequently, under these conditions, the supratransmission effect is not observed.

At a higher driving amplitude of $A = 0.28$ Å, the temporal evolution of the kinetic energy exhibits a markedly different behavior as shown in Fig. 1b. Specifically, in the frequency range of 9.93 – 10.5 THz, an initial stage of gradual energy pumping is observed, corresponding to a nearly linear increase in kinetic energy, followed by a sharp rise. Subsequently, a distinct kink appears in the $E_k(t)$ curves, after which the energy continues to increase at a rate comparable to that before the kink. This stage is typically followed by a transient saturation and a subsequent renewed growth in energy. In this amplitude range, a supratransmission effect is observed, accompanied by the generation of two discrete breathers that propagate away from their point of origin in opposite directions. To accurately capture this process, the computational cell was chosen to be sufficiently elongated along the x-axis (the direction of discrete breathers' propagation) allowing the generated breathers to travel without interacting with their periodic images and enabling the subsequent formation of new breathers. At higher frequencies of 10.06 and 10.09 THz, no significant increase in kinetic energy occurs, and the supratransmission effect is no longer present (see Fig. 1b).

Figure 2 shows the temporal evolution of the potential energy within the computational supercell, demonstrating the formation and propagation of a discrete breather originating from two driving atoms. The results are given for driving amplitude of $A = 0.25$ Å and frequency of $\omega = 9.97$ THz. At 0.5 ps, only the nearest atoms are excited, corresponding to the initial stage of energy pumping. At 4.25 ps, two discrete breathers are formed, which corresponds with the kink in the kinetic energy curve. These breathers then propagate away from their origin in opposite directions along the close-packed atomic rows. After that, continued energy pumping results in the formation of another pair of discrete breathers, which again move in opposite directions followed the first ones. This process repeats periodically, indicating the sustained generation of localized vibrational modes under high-amplitude excitation.

From the analysis of the results presented above, it follows that there exists a critical frequency of the driven atoms, ω_c, below which the supratransmission effect occurs and above which it does not. In other words, when the driving frequency exceeds the critical value, i. e., $\omega > \omega_c$, no significant energy transfer to the lattice takes place, resulting in a plateau in the $E(t)$ dependence (Fig. 1b). Conversely, when the frequency is below the critical threshold, i. e., $\omega < \omega_c$, the kinetic energy of the system increases due to the gradual transfer of energy from the driven atoms to the lattice.

Figure 3 displays the dependence of the critical frequency on the amplitude of the driven atoms. At low amplitudes, the critical frequencies are located near the upper edge of the phonon spectrum. As the amplitude increases, the critical frequency rises almost linearly with the driving amplitude. Thus, the supratransmission regime is realized below the curve (in the green-shaded region in Fig. 3), while above this curve the system remains in a non-transmitting state.

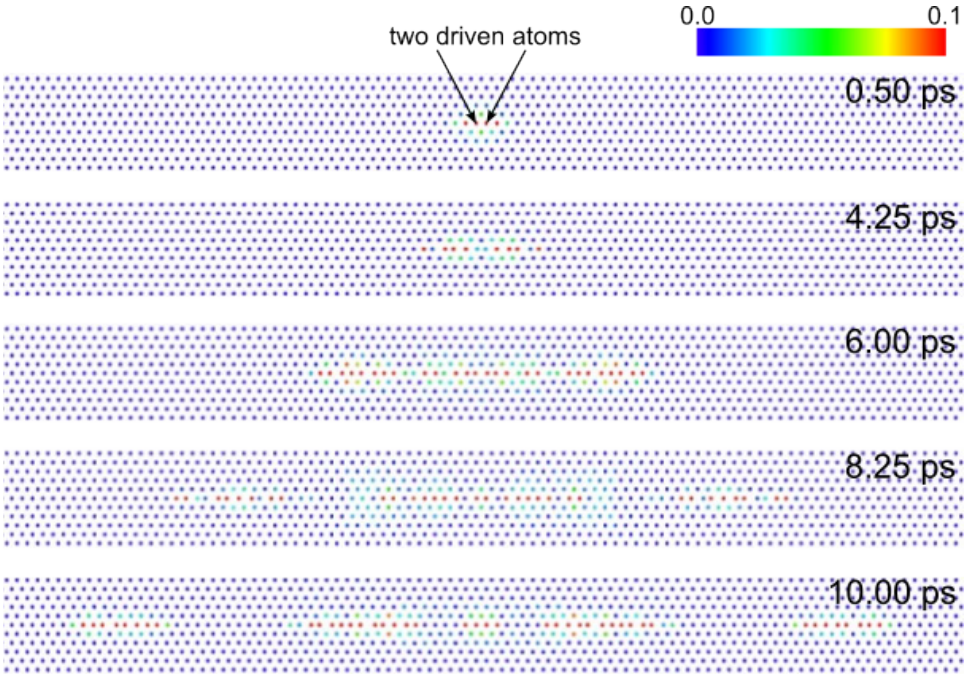

Fig. 2. (Color online) Potential energy maps (eV) in the computational supercell at different times (shown on the right). The driving amplitude is $A = 0.25$ Å and the frequency is $\omega = 9.97$ THz. The two driven atoms are indicated by black arrows. For clarity, only a part of the computational cell is displayed.

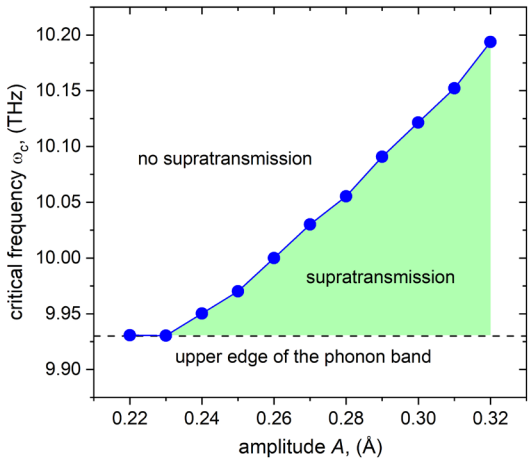

Fig. 3. (Color online) The critical value of the frequency as a function of driving amplitude A. The horizontal dashed line demonstrates the upper edge of the phonon spectrum. The green-shaded region below the curve corresponds to the frequency-amplitude range in which the supratransmission effect is observed. The solid lines connecting the data points are provided as visual guide.

4. Discussion

The supratransmission effect is observed only within a relatively narrow range of driving amplitudes and frequencies. Identifying these ranges requires systematic exploration of various amplitude-frequency combinations. Moreover, the critical parameters depend slightly on the specific interatomic potential employed, since different potentials reproduce somewhat different upper boundaries of the phonon spectrum and exhibit varying bond stiffnesses.

The dependence of the critical frequency on the driving amplitude is approximately linear. However, this relationship holds only up to a certain threshold amplitude. Beyond this point, the atomic displacements become large enough to drive atoms far from their equilibrium lattice sites, potentially leading to the formation of point defects (vacancy-interstitial pairs) and enhanced dissipation of vibrational energy.

Analysis of the atomic configurations reveals that when the driving frequency approaches the critical value from below, regular discrete breathers are generated, propagating predominantly along the *x*-axis. In contrast, as the driving frequency nears the upper limit of the phonon spectrum, the emitted localized modes become increasingly irregular and less stable.

At present, a direct comparison with results from other studies on the supratransmission effect is not feasible, as the present work provides the first results for three-dimensional fcc nickel. Previous investigations have focused primarily on two-dimensional lattices and have typically employed pairwise interatomic potentials, which do not capture the full complexity of metallic bonding [22–26]. The supratransmission in three-dimensional systems has been examined previously for Pt_3Al alloy using embedded-atom method potential [27,28]. In those studies, driving force was applied to several atomic layers rather than to individual atoms, as in the present work. The authors reported the existence of a specific range of amplitudes and frequencies within which supratransmission occurs, accompanied by the emission of quasi-breathers propagating along preferred crystallographic directions determined by the lattice symmetry. Despite the differences in crystal structure and excitation scheme, the results obtained in the present study for pure nickel show good qualitative agreement with the findings for Pt_3Al alloy.

A potential continuation of this study could involve investigating the supratransmission effect in other metals with a fcc lattice to explore whether the observed phenomenon is consistent across different materials with similar crystal structures. In addition, it would be interesting to study the supratransmission effect in various carbon compounds and silicene, which are of great interest from both fundamental and applied perspectives [38–41]. Furthermore, studying the influence of phase shift between the driven atoms could provide insights into its role in enabling or modulating the supratransmission effect, potentially revealing new conditions or mechanisms that govern this nonlinear phenomenon.

5. Conclusions

For the first time, molecular dynamics simulations of the energy transfer in a three-dimensional fcc lattice of nickel driven harmonically through a pair of neighboring atoms at frequencies outside the phonon spectrum of the crystal was investigated. The critical driving frequency as a function of the driving amplitude was determined. When the frequency is below the threshold value, the energy is transmitted from the driven particles into the lattice, which is accompanied by emission of discrete breathers in opposite directions along the close-packed atomic rows. When the frequency exceeds the critical value, no supratransmission takes place.

References

1. A.S. Dolgov, On localization of oscillations in nonlinear crystal structure, Sov. Phys.-Solid State 28 (1986) 907.
2. A.J. Sievers, S. Takeno, Intrinsic localized modes in anharmonic crystals, Phys. Rev. Lett. 61 (1988) 970–973.
3. J.B. Page, Asymptotic solutions for localized vibrational-modes in strongly anharmonic periodic-systems, Phys. Rev. B 41 (1990) 7835–7838.
4. S. Flach, Energy properties of discrete breathers, Physica D 113 (1998) 184–190.
5. S.V. Dmitriev, E.A. Korznikova, Y.A. Baimova, M.G. Velarde, Discrete breathers in crystals, Physics — Uspekhi 59 (2016) 446–461.
6. M.E. Manley, M. Yethiraj, H. Sinn, H.M. Volz, A. Alatas, J.C. Lashley, W.L. Hults, G.H. Lander, D.J. Thoma, J.L. Smith, Intrinsically localized vibrations and the mechanical properties of α-uranium, J. Alloy Compd. 444 (2007) 129–132.
7. E.A. Korznikova, A.Y. Morkina, M. Singh, A.M. Krivtsov, V.A. Kuzkin, V.A. Gani, Y.V. Bebikhov, S.V. Dmitriev, Effect of discrete breathers on macroscopic properties of the Fermi-Pasta-Ulam chain, Eur. Phys. J. B 93 (2020) 123.
8. J. Wang, S.V. Dmitriev, D. Xiong, Thermal transport in long-range interacting Fermi-Pasta-Ulam chains, Physical Review Research 2 (2020) 013179.

9. B. Mihaila, C. P. Opeil, F. R. Drymiotis, J. L. Smith, J. C. Cooley, M. E. Manley, A. Migliori, C. Mielke, T. Lookman, A. Saxena, A. R. Bishop, K. B. Blagoev, D. J. Thoma, J. C. Lashley, B. E. Lang, J. Boerio-Goates, B. F. Woodfield, G. M. Schmiedeshoff, Pinning frequencies of the collective modes in α-uranium, Phys. Rev. Lett. 96 (2006) 076401.
10. D. Saadatmand, D. X. Xiong, V. A. Kuzkin, A. M. Krivtsov, A. V. Savin, S. V. Dmitriev, Discrete breathers assist energy transfer to ac-driven nonlinear chains, Physical Review E 97 (2018) 022217.
11. O. V. Bachurina, A. A. Kudreyko, D. V. Bachurin, Influence of two-dimensional discrete breathers on the macroscopic properties of fcc metals, Eur. Phys. J. B, 98 (2025) 27.
12. O. V. Bachurina, A. A. Kudreyko, S. V. Dmitriev, D. V. Bachurin, Impact of delocalized nonlinear vibrational modes on the properties of NiTi, Phys. Lett. A 555 (2025) 130769.
13. O. V. Bachurina, R. T. Murzaev, S. A. Shcherbinin, A. A. Kudreyko, S. V. Dmitriev, D. V. Bachurin, Delocalized nonlinear vibrational modes in Ni_3Al, Commun. Nonlinear Sci. 132 (2024) 107890.
14. A. Upadhyaya, M. N. Semenova, A. A. Kudreyko, S. V. Dmitriev, Chaotic discrete breathers and their effect on macroscopic properties of triangular lattice, Commun. Nonlinear Sci. 112 (2022) 106541.
15. M. Singh, A. Y. Morkina, E. A. Korznikova, V. I. Dubinko, D. A. Terentiev, D. X. Xiong, O. B. Naimark, V. A. Gani, S. V. Dmitriev, Effect of discrete breathers on the specific heat of a nonlinear chain, J. Nonlinear Sci. 31 (2021) 12.
16. J. E. Macías-Díaz, A. Puri, An application of nonlinear supratransmission to the propagation of binary signals in weakly damped, mechanical systems of coupled oscillators, Phys. Lett. A 366 (2007) 447 – 450.
17. D. Chevriaux, R. Khomeriki, J. Leon, Theory of a Josephson junction parallel array detector sensitive to very weak signals, Phys. Rev. B 73 (2006) 214516.
18. F. Tao, W. Z. Chen, J. T. Pan, W. Xu, S. D. Du, Experimental observation on asymmetric energy flux within the forbidden frequency band in the *LC* transmission line, Chaos Soliton Fract. 45 (2012) 810 – 814.
19. J. G. Caputo, J. Leon, A. Spire, Nonlinear energy transmission in the gap, Phys. Lett. A 283 (2001) 129 –135.
20. F. Geniet, J. Leon, Energy transmission in the forbidden band gap of a nonlinear chain, Phys. Rev. Lett. 89 (2002) 134102.
21. F. Geniet, J. Leon, Nonlinear supratransmission, J. Phys-Condens Mat. 15 (2003) 2933 – 2949.
22. J. E. Macias-Diaz, Numerical study of the process of nonlinear supratransmission in Riesz space-fractional sine-Gordon equations, Commun Nonlinear Sci, 46 (2017) 89 –102.
23. J. E. Macías-Díaz, J. Ruiz-Ramírez, L. A. Flores-Oropeza, Computational study of the transmission of energy in a two-dimensional lattice with nearest-neighbor interactions, Int. J. Mod. Phys. C 20 (2009) 1933 –1943.
24. J. Ruiz-Ramírez, J. E. Macías-Díaz, On the propagation of binary signals in a two-dimensional nonlinear lattice with nearest-neighbor interactions, J. Nonlinear Math Phy. 17 (2010) 127–136.
25. D. U. Abdullina, E. K. Naumov, Y. Bebikhov, M. N. Semenova, A. A. Kudreyko, S. Dmitriev, Supratransmission in a β-FPUT square lattice, Phys. Lett. A 550 (2025) 130587.
26. Y. V. Bebikhov, E. K. Naumov, M. N. Semenova, S. V. Dmitriev, Discrete breathers in a β-FPUT square lattice from in-band external driving, Commun. Nonlinear Sci. 132 (2024) 107897.
27. A. I. Cherednichenko, P. V. Zakharov, M. D. Starostenkov, M. O. Sysoeva, A. M. Eremin, Nonlinear supratransmission in a Pt_3Al crystal at intense external influence, Comput. Res. Model. 11 (2019) 109 –117. (in Russian)
28. P. V. Zakharov, E. A. Korznikova, A. A. Izosimov, Kochkin, The influence of crystal anisotropy on the characteristics of solitary waves in the nonlinear supratransmission effect: molecular dynamic modeling, Computation, 11 (2023) 193.
29. P. V. Zakharov, The effect of nonlinear supratransmission in discrete structures: a review, Comput. Res. Model. 15 (2023) e599 – e617.
30. LAMMPS, Available online
31. S. A. Etesami, E. Asadi, Molecular dynamics for near melting temperatures simulations of metals using modified embedded-atom method, J. Phys. Chem. Solids 112 (2018) 61 – 72.
32. H. S. M. Phuong, N. T. H. Trung, M. D. Starostenkov, Thermo-mechanical properties of random ternary alloy V-5Cr-5Ti, Letters on Materials 15 (1) (2025) 36 – 42.
33. E. A. Rozhnova, L. R. Safina, K. A. Krylova, Tensile strength and nanohardness of Cu with graphene/Cu composite coating: atomistic simulation, Letters on Materials 15 (2) (2025) 112 –119.
34. H. Sharifi, C. D. Wick, The effects of the W on the phase segregation and shear strength of CrNiCo: A molecular dynamics study, Comp. Mater. Sci. 253 (2025) 113877.
35. S. V. Starikov, N. Y. Lopanitsyna, D. E. Smirnova, S. V. Makarov, Atomistic simulation of Si-Au melt crystallization with novel interatomic potential, Comp. Mater. Sci. 142 (2018) 303 – 311.
36. S. M. Foiles, M. I. Baskes, M. S. Daw, Embedded-atom-method functions for the fcc metals Cu, Ag, Au, Ni, Pd, Pt, and their alloys, Phys. Rev. B 33 (1986) 7983 – 7991.
37. X. W. Zhou, H. N. G. Wadley, R. A. Johnson, D. J. Larson, N. Tabat, A. Cerezo, A. K. Petford-Long, G. D. W. Smith, P. H. Clifton, R. L. Martens, T. F. Kelly, Atomic scale structure of sputtered metal multilayers, Acta Mater. 49 (2001) 4005 – 4015.
38. O. E. Glukhova, M. M. Slepchenkov, Effect of LaB6 nanoparticles on the electronic and emission properties of single-walled carbon nanotubes/graphene hybrid 1D nanomaterial, Letters on Materials 13 (4) (2023) 312 – 316. DOI: 10.22226/2410-3535-2023-4-312-316 Webpage
39. V. A. Greshnyakov, V. V. Pavlik, Calculations of the structure and properties of autointercalated graphyne layers, Letters on Materials 13 (4) (2023) 323 – 328. DOI: 10.22226/2410-3535-2023-4-323-328 Webpage
40. P. V. Polyakova, L. K. Galiakhmetova, R. T. Murzaev, D. S. Lisovenko, J. A. Baimova, Elastic properties of diamane, Letters on Materials 13 (2) (2023) 171–176.
41. A. K. Akhunova, R. T. Murzaev, Deformation behaviour of silicene with dislocation dipoles under uniaxial tension, Letters on Materials 15 (3) (2025) 207 – 212.